



Contents lists available at ScienceDirect

Journal of the Taiwan Institute of Chemical Engineers

journal homepage: www.elsevier.com/locate/jtice

Fabrication of reduced glutathione functionalized iron oxide nanoparticles for magnetic removal of Pb(II) from wastewater

Piao Xu^{a,b}, Guang Ming Zeng^{a,b,*}, Dan Lian Huang^{a,b,*}, Ming Yan^{a,b}, Ming Chen^{a,b}, Cui Lai^{a,b}, Hui Jiang^{a,b}, Hai Peng Wu^{a,b}, Guo Min Chen^{a,b}, Jia Wan^{a,b}^a College of Environmental Science and Engineering, Hunan University, Changsha 410082, PR China^b Key Laboratory of Environmental Biology and Pollution Control (Hunan University), Ministry of Education, Changsha 410082, PR China

ARTICLE INFO

Article history:

Received 1 February 2016

Revised 21 November 2016

Accepted 25 November 2016

Available online xxx

Keywords:

Iron oxide magnetic nanoparticles

Pb(II)

Silanization

Adsorption

Reduced glutathione

ABSTRACT

In this study, a novel nanoadsorbent (Fe₃O₄-SiO₂-GSH MNPs) based on iron oxide magnetic nanoparticles (Fe₃O₄ MNPs), coated with SiO₂ shells and further modified via reduced glutathione (GSH), was successfully synthesized and applied for Pb(II) removal. Characterization results suggested that the prepared nanoadsorbents were in uniform size and provided numerous adsorption sites for Pb(II), nanoparticles could be convenient separated with the help of external magnet due to their superparamagnetism. Adsorption results showed that the prepared nanoadsorbents exhibited excellent adsorption capacity, even at a large range of Pb(II) concentrations and ionic strength scope. Kinetic of the Pb(II) adsorption was found to follow pseudo-second-order rate equation. Adsorption isotherm data was best fitted to Freundlich model ($R^2 = 0.9888-0.9959$), and the maximal Pb(II) adsorption capacities were calculated as 298.87, 332.44 and 357.37 mg g⁻¹, at 298, 303 and 308 K, respectively. Based on the efficient Pb(II) adsorption ability and reusability studies, Fe₃O₄-SiO₂-GSH MNPs were confirmed to be a promising candidate for Pb(II) removal from industrial effluents.

© 2016 Taiwan Institute of Chemical Engineers. Published by Elsevier B.V. All rights reserved.

1. Introduction

Concern over the presence of heavy metals in the environment is increasing nowadays, owing to their long-term and serious toxicity to human and ecosystems. Heavy metals are widely existed in surface water, groundwater, and even in drinking water, discharging from mining operations, tanneries, electronics, electroplating, as well as textile mill products [1,2]. Various technologies have been applied for heavy metal containing wastewater treatment, such as chemical precipitation, reverse osmosis, ion-exchange, filtration, electrodialysis, adsorption, and so on [3,4]. Among these, adsorption technique is widely applied due to high efficiency, low cost, easy operation and applicable at relative low concentrations [5–7].

In recent years, alternative technologies using nanomaterials have attracted significant attention on environmental remediation. Currently, some nanocomposite adsorbents, such as carbon nanotubes, iron oxide nanoparticles, graphene, and zero valent iron, are commercially available for field application in the removal of heavy metals [8–11]. Such novel structures contributed to favorable

adsorption capacities as well as remarkably accelerated adsorption rates, via facilitating the mass transportation of the targets, owing to its nano-size and large surface areas.

Recent advances suggested that many of the issues in wastewater could be resolved or greatly ameliorated using iron oxide magnetic nanoparticles (Fe₃O₄ MNPs). A large number of studies have been conducted dealing with wastewater based on Fe₃O₄ MNPs, due to their high adsorption capacities, highly efficient and cost-effective, easy and complete magnetic separation for reusability [12–14]. Nevertheless, field application of bare Fe₃O₄ MNPs is limited. The limited application might be ascribed to the inevitable challenges of nanoadsorbents, such as aggregation and limited surface sites [15]. Taking advantage of its high superficial area and acceptability of various molecules, surface modification is desirable for effective application, via providing specific adsorption sites for metal uptake [16,17]. A great deal of effort has been devoted to the preparation of core-shell Fe₃O₄ MNPs or surface coated Fe₃O₄ MNPs to expand the application performance [18–21]. For example, nZVI-Fe₃O₄/C composites and aluminon-functionalized magnetic nanoparticles were successful synthesized and efficient for Cr(VI) removal [19,21]. The nature of the magnetic core and the surface coatings therefore serves for the higher performance and improved applicability in wastewater treatment.

* Corresponding authors. Fax: +86 731 88823701.

E-mail addresses: zgming@hnu.edu.cn (G.M. Zeng), huangdanlian@hnu.edu.cn (D.L. Huang).<http://dx.doi.org/10.1016/j.jtice.2016.11.031>

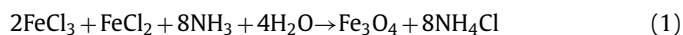
1876-1070/© 2016 Taiwan Institute of Chemical Engineers. Published by Elsevier B.V. All rights reserved.

Here, reduced glutathione (GSH) were grafted on the silanized Fe_3O_4 MNPs for the preparation of $\text{Fe}_3\text{O}_4\text{-SiO}_2\text{-GSH}$ MNPs. GSH, as a tri-peptide and an effective acceptor of heavy metal ions, has been widely used in the detoxification of metals via formation of metal-thiol complex (such as Pb-GSH) [22,23]. As-obtained functionalized Fe_3O_4 MNPs were systematically investigated for their applications as Pb(II) nanoadsorbents. Experimental factors, such as pH, contact time, nanoadsorbent dosage, initial Pb(II) concentration and ionic strength, were analyzed through a batch equilibrium technique. Moreover, reusability of the prepared nanoadsorbent was examined. Efforts were devoted to elucidate the adsorption ability and recyclability of the prepared nanoadsorbents.

2. Materials and methods

2.1. Preparation of Fe_3O_4 MNPs

Fe_3O_4 MNPs were prepared by co-precipitation of Fe(II) and Fe(III) in ammonia solution, according to our previous study [8]. The co-precipitation of Fe(II) and Fe(III) was done in the mentioned conditions according to Eq. (1) [13]. Firstly, $\text{FeCl}_3\cdot 6\text{H}_2\text{O}$ (12.75 g) and $\text{FeCl}_2\cdot 4\text{H}_2\text{O}$ (4.5 g) were dissolved in 57 ml HCl solution (0.4 M), and then added dropwise into 562 ml NH_4OH (0.7 M) under strong mechanical agitation condition for 30 min under N_2 stream. Ultrapure water used for both HCl and NH_4OH solution were previously flushed with N_2 for 10 min. Then, the formed particles were washed three times with distilled water, and dispersed into 100 ml ultrapure water (~ 5 g Fe_3O_4 MNPs/100 ml). All chemicals were of analytical grade without further purification. Ultrapure water was used for the preparation of all the solutions throughout this study.



2.2. Functionalization of Fe_3O_4 MNPs

80 ml of as-prepared Fe_3O_4 MNPs suspension was dispersed in 150 ml ethanol solution, stirring for 15 min. Then 50 ml ammonia solution (0.7%, volume ratio) was added and stirring for another 15 min under N_2 stream. Next, 22 mM of tetraethylorthosilicate (TEOS) was added to the solution for 1.5 h, thereafter 20 mM of 3-aminopropyltriethoxysilane (APTES) was added and stirring for another 1.5 h. All the operation was conducted under N_2 atmosphere at room temperature (25–30°C). The prepared $\text{Fe}_3\text{O}_4\text{-SiO}_2$ MNPs were washed with ethanol and de-ionized water for three times and then quantified to 100 ml with ultrapure water. After that, 80 ml of above $\text{Fe}_3\text{O}_4\text{-SiO}_2$ MNPs suspension was then dispersed in 450 ml deoxidized ultrapure water containing of 3.0990 g GSH under strong mechanical stirring for 4 h at room temperature. $\text{Fe}_3\text{O}_4\text{-SiO}_2\text{-GSH}$ MNPs were then separated by soft magnetic decantation and washed again with deoxidized water to the neutral.

2.3. Structural and chemical characterization of nanoadsorbents

Field emission scanning electron microscopy (FSEM, Hitachi SU8010) was performed to characterize general morphology of the nanoparticles. X-ray powder diffraction (XRD) patterns were obtained on a D/Max-RB X-ray diffractometer (Ultima IV) using $\text{Cu}_{K\alpha}$ radiation ($\lambda = 0.1541$ nm) at 40 kV and 40 mA. The infrared spectroscopy was recorded by a Fourier transform infrared spectrophotometer (FTIR) (Nicolet, Nexus-670) with crystalline KBr in the range of 4000–400 cm^{-1} . Hysteresis loops were performed via vibrating sample magnetometer (VSM, MPMS SQUID VSM) varying from -3 to 3 kOe at 300 K. The specific surface area of the functionalized MNPs was determined with nitrogen adsorption-desorption Brunauer, Emmett, and Teller (BET) measurements (Nova 2200e).

2.4. Batch experiments of Pb(II) adsorption

For adsorption investigation, a known amount of nanoadsorbents were added into a 50 ml Pb(II) -containing solution over a period of time on a shaker at 150 rpm. The Pb(II) adsorption was studied as functions of pH (2.0–5.5), contact time (0–180 min), temperature (25–35°C), adsorbent dosage (0.2–2.0 g l^{-1}), initial Pb(II) concentration (0–500 mg l^{-1}) and ionic strength (0.025–0.2 mM NaCl). All the adsorption experiments were carried out in duplicate. The concentrations of Pb(II) after adsorption (filtered with 0.45 μm filter membrane) was determined by atomic absorption spectrometer (Agilent 3510, USA). The amount of Pb(II) ions adsorbed per unit mass of the nanoadsorbent was evaluated as Eq. (2):

$$q_t = (c_0 - c_t)V/W \quad (2)$$

where q_t (mg g^{-1}) is the amount adsorbed per gram of adsorbent at time t (min), c_0 is the initial concentration of Pb(II) (mg l^{-1}), c_t is the residual Pb(II) concentration at time t of adsorption (mg l^{-1}), W is the mass of the adsorbent used (g), and V (l) is the initial volume of the Pb(II) solution.

2.5. Desorption and reusability studies

Desorption study was conducted by adding 25 ml of HNO_3 solution (0.1 M) to the Pb(II) -adsorbed $\text{Fe}_3\text{O}_4\text{-SiO}_2\text{-GSH}$ MNPs and shaking at 150 rpm for 1 h. After desorption, the solid phase nanoadsorbents were collected by magnetic decantation and washed with ultrapure water for three times. 50 ml of Pb(II) solution (100 mg l^{-1} , pH 5.5) was added and adsorbed for 120 min. The reusability was checked by following the above adsorption-desorption process for six cycles. Illustration of the synthesis processes and application of $\text{Fe}_3\text{O}_4\text{-SiO}_2\text{-GSH}$ MNPs is presented in Fig. 1.

3. Results and discussion

3.1. Characterization of magnetic nanoparticles

FSEM image of the Fe_3O_4 MNPs shown in Fig. 2a demonstrated that Fe_3O_4 MNPs were uniformly distributed with uniform size. The nanoparticles were almost spherical and cubic shaped. After modified with SiO_2 and GSH, no obvious morphology variation observed. $\text{Fe}_3\text{O}_4\text{-SiO}_2\text{-GSH}$ MNPs were spherical shaped and finely dispersed. Fig. 3a shows the XRD data for the synthesized Fe_3O_4 MNPs and $\text{Fe}_3\text{O}_4\text{-SiO}_2\text{-GSH}$ MNPs. The obtained peak at $2\theta = 30.09^\circ$, 35.44° , 43.07° , 53.44° , 56.96° and 62.55° , correspond to the cubic structure of magnetite Fe_3O_4 . The crystalline size of Fe_3O_4 MNPs was calculated as about 39.3 nm, according to Scherrer equation ($D = k\lambda/\beta\cos\theta$) [24]. After coating with the SiO_2 and GSH, the diffraction pattern of $\text{Fe}_3\text{O}_4\text{-SiO}_2\text{-GSH}$ MNPs showed a reflection characteristic of amorphous SiO_2 ($2\theta = 26.57^\circ$) in addition to the Fe_3O_4 reflections. Additionally, the average crystal size of $\text{Fe}_3\text{O}_4\text{-SiO}_2\text{-GSH}$ MNPs was 45.3 nm deduced from Scherrer formula.

The FTIR patterns shown in Fig. 3b demonstrated the strong peak appeared at 567 cm^{-1} corresponding to Fe–O bond of bulk magnetite band. Meanwhile, a broad absorption band around 3520 cm^{-1} was also observed, which assigned to –OH at the surface of Fe_3O_4 MNPs. Wide band around 3520 cm^{-1} disappeared after silanization, due to the coupling with Si–O at the surface of Fe_3O_4 MNPs ($\text{Fe}_3\text{O}_4\text{-SiO}_2$ MNPs). Indeed, as shown in Fig. 3b, the introduction of TEOS and APTES was further confirmed by the bands at 1115 cm^{-1} and 1039 cm^{-1} represented the Si–O groups. Most importantly, a new band appeared at 803 cm^{-1} assigned to

Download English Version:

<https://daneshyari.com/en/article/4998767>

Download Persian Version:

<https://daneshyari.com/article/4998767>

[Daneshyari.com](https://daneshyari.com)